THE ASTROPHYSICAL JOURNAL, 549:L265–L268, 2001 March 10

UNIFIED ELECTRONIC RECOMBINATION OF Ne-LIKE Fe XVII: IMPLICATIONS FOR MODELING X-RAY PLASMAS

ANIL K. PRADHAN AND SULTANA N. NAHAR
Department of Astronomy, Ohio State University, 140 West 18th Avenue, Columbus, OH 43210
AND
HONG LIN ZHANG
Los Alamos National Laboratory, MS F663, Los Alamos, NM 87545
Received 2000 November 27; accepted 2001 January 19; published 2001 February 27

ABSTRACT

Unified recombination cross sections and rates are computed for (e + Fe XVIII) → Fe XVII including nonresonant and resonant (radiative recombination [RR] and dielectronic recombination [DR]) processes in an ab initio manner with relativistic fine structure. The highly resolved theoretical cross sections exhibit considerably more resonance structures than observed in the heavy-ion storage ring measurements at Heidelberg, Germany. Nonetheless, the detailed resonance complexes agree well with experimental results, and the unified rates agree with the sum of experimentally derived DR and theoretical RR rates to ~20%, within experimental or theoretical uncertainties. Theoretical results may provide estimates of field ionization of Rydberg levels close to the DR peak and nonresonant background contributions particularly close to the RR peak as $E \rightarrow 0$. More generally, the unified results avoid the physical and practical problems in astrophysical models inherent in the separation of electronic recombination into RR and DR on the one hand and further subdivision into low-energy $\Delta n = 0$ DR and high-energy $\Delta n > 0$ DR in photoionized and collisionally ionized X-ray plasmas on the other hand.

Subject headings: atomic data — atomic processes — line: formation — X-rays: general

1. INTRODUCTION

The *Chandra X-Ray Observatory* and the *XMM-Newton* are observing a variety of sources (Canizares et al. 2000; Predehl et al. 2000)[1] with wide-ranging plasma conditions. The analysis requires astrophysical models (e.g., Kallman 1995; Brickhouse, Raymond, & Smith 1995) whose accuracy depends on the atomic cross sections for collisional and radiative processes such as electron impact excitation, photoionization, and recombination. K- and L-shell iron ions are among the most prominent atomic species in many sources, such as active galactic nuclei (Ogle et al. 2000), stellar coronae and winds (Schulz et al. 2000), and cooling flows in clusters of galaxies (Fabian et al. 2001). Excitation, photoionization, and recombination of Ne-like Fe XVII are of particular interest, as this ion is a strong X-ray radiator owing to a multitude of L-shell excitations at $T < 1$ keV.

Although most of these atomic parameters are obtained theoretically, those need to be benchmarked against available experimental measurements. In recent years, there has been considerable progress in both theoretical and experimental methods. High-resolution electron-ion recombination measurements on ion storage rings show very detailed resonance structures in the low-energy region usually accessible in experiments (e.g., Mannervik et al. 1997; Kilgus et al. 1992). Recently, such measurements have been done for (e + Fe XVIII) → Fe XVII (Savin et al. 1997, 1999) in the low-energy region dominated by $\Delta n = 0$ resonances. The experimental results naturally measured the combined nonresonant and resonant contributions. These were then processed to separate the background and extract the resonance contributions (dielectronic recombination [DR]) by fitting with an experimentally deduced beam shape function. Savin et al. find that their inferred DR rates from low-energy measurements differ from previous theoretical calculations by up to a factor of 2 or more. Their best agreement of ≈30% is with multiconfiguration Dirac-Fock (MCDF) and Breit-Pauli calculations in the isolated resonance approximation. The comparison of derived DR rates for individual resonances (or blends) showed varying levels of agreement.

As the (e + ion) recombination is unified in nature, it is theoretically desirable to consider the nonresonant and resonant processes (radiative recombination [RR] and DR) together. A unified theoretical formulation has been developed (e.g., Nahar & Pradhan 1994, hereafter NP94; Zhang, Nahar, & Pradhan 1999, hereafter Z99), including relativistic fine structure (Zhang & Pradhan 1997), and used to compute cross sections and rates for many atomic systems, such as the K-shell systems C IV–C V and Fe XXIV–Fe XXV of interest in X-ray spectroscopy (Nahar, Pradhan, & Zhang 2000, 2001, hereafter N00 and N01). The unified results may be directly compared with experimental results, without the need to separate RR and DR. In this Letter we present new results for the L-shell system Fe XVII and show that the unified cross sections and rates are not only in very good agreement with experimental results but may also be used to study important physical effects, such as ionization of high-Rydberg bound and autoionizing levels. More generally, the results demonstrate that the unified calculations avoid the basic inconsistency and incompleteness of photoionization and recombination data for the modeling of laboratory and astrophysical plasma sources.

2. THEORY AND COMPUTATIONS

From a quantum mechanical point of view, photoionization and recombination may be treated in a self-consistent manner by considering the same coupled eigenfunction expansion for the core (photoionized or recombining) ion. For Fe XVII we write

$$\Psi(E;\ e + \text{Fe XVIII}) = \sum_i \chi_i(\text{Fe XVIII})\theta_i(e) + \sum_j c_j \Phi_j(\text{Fe XVII}), \quad (1)$$

where Ψ denotes both the bound ($E < 0$) and the continuum

[1] See also http://heasarc.gsfc.nasa.gov/docs/heasarc/atomic/proceed.html.

($E > 0$) states of Fe XVII, expanded in terms of the core ion eigenfunctions χ_i (Fe XVIII); Φ_j are correlation functions. The close-coupling approximation, based on the efficient *R*-matrix method (Burke, Hibbert, & Robb 1971), and its relativistic Breit-Pauli extension (Scott & Taylor 1982), enables a solution for the total Ψ, with a suitable expansion over the χ_i. The Breit-Pauli *R*-matrix (BPRM) method has been extensively employed for electron impact excitation under the Iron Project (Hummer et al. 1993; Berrington, Eissner, & Norrington 1995). The extension of the BPRM formulation to unified electronic recombination (e.g., Z99; N00; N01) and theoretically self-consistent calculations of photoionization and recombination is sketched below.

Resonant and nonresonant electronic recombination takes place to an infinite number of bound levels of the (e + ion) system. These are divided into two groups: (1) the low-n ($n \le n_0 \approx 10$) levels, considered via detailed close-coupling calculations for photorecombination, with highly resolved delineation of autoionizing resonances, and (2) the high-n ($n_0 \le n \le \infty$) recombining levels via DR, neglecting the background. In previous works (e.g., Z99), it has been shown that in the energy region corresponding to group 1, below the threshold for DR, the nonresonant contribution is negligible. The DR cross sections converge onto the electron impact excitation cross section at the threshold ($n \to \infty$, as required by unitarity, i.e., conservation of photon and electron fluxes). This theoretical limit is an important check on the calculations and enables a determination of field ionization of Rydberg levels of resonances contributing to DR.

Complete details of the extensive BPRM calculations for photoionization and recombination of Fe XVII will be presented elsewhere. The multiconfiguration target eigenfunctions χ_i (Fe XVIII) (eq. [1]) are obtained from an atomic structure calculation with five spectroscopic configurations, $2s^2 2p^5$, $2s2p^6$, $2s^2 2p^4 3s$, $3p$, $3d$, and a number of correlation configurations, optimized over the resulting 60 fine-structure levels using the program SUPERSTRUCTURE (Eissner, Jones, & Nussbaumer 1974). In the low-energy region of interest in the present work, and in experiments, the levels are $2s^2 2p^5(^2P^o_{1/2,\,3/2})$ and $2s2p^6(^2S_{1/2})$. The computed target level energies agree with the observed ones to less than 1%, and the oscillator strengths agree with those tabulated by the National Institute of Standards and Technology[2] to less than 5%.

We consider photorecombination cross sections for 359 levels of Fe XVII. Total angular symmetries with $J \le 7$ (odd and even) and levels with $\nu \le 10.0$ (ν is the effective quantum number) are included in the photoionization calculations. The photorecombination cross sections are obtained via detailed balance using radiatively damped photoionization cross sections (Pradhan & Zhang 1997). Resonances with higher symmetries make a negligible contribution. For $10 < \nu \le \infty$, the calculations are carried out by extending the Bell & Seaton (1985) theory of DR. As the DR calculations are an extension of the electron-scattering calculations (e.g., NP94; Z99), the DR and the electron impact cross sections are obtained in a self-consistent manner satisfying the unitarity of the extended electron-photon *S*-matrix.

3. RESULTS

Figure 1*a* shows the total unified recombination cross section σ_{RC} for Fe XVII. It shows photorecombination into all 359 levels

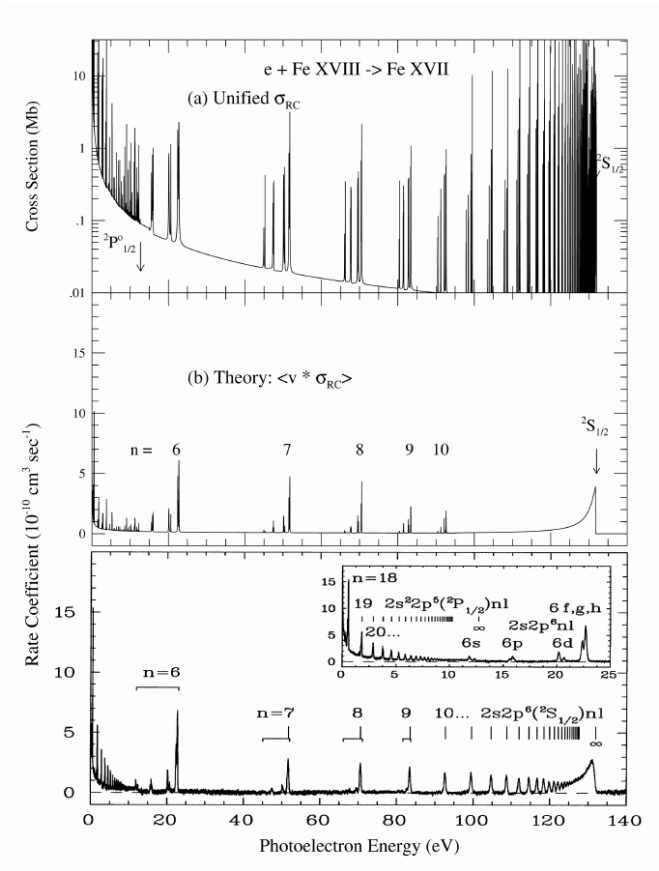

FIG. 1.—Unified recombination cross section σ_{RC} for Fe XVII. (*a*) Narrow Rydberg resonances converging to the $2s^22p^5(^2P^o_{1/2})$ threshold at 12.7 eV and the *n*-complexes belonging to the $2s2p^6(^2S_{1/2})$ threshold are delineated. The high-*n* DR resonances are shown in the region $E > 90$ eV. (*b*) Theoretical rate coefficients $\langle v\sigma_{RC}\rangle$ convolved over a Gaussian beam shape, compared to experimental data in the lower panel (Savin et al. 1999). The averaged theoretical DR contribution for resonances with $10 < \nu \le \infty$ below the $^2S_{1/2}$ threshold is analytically computed exactly.

of Fe XVII with $\nu \le 10$ ($E \approx 90$ eV) and DR for $10 < \nu < \infty$ up to $E = 132.0063$ eV, the $^2S_{1/2}$ threshold. A Rydberg series of resonances converges onto the first excited level $^2P^o_{1/2}$ at 12.7 eV followed by the stronger series $n \ge 6$ on the $^2S_{1/2}$ level at 132.0063 eV. It is evident from Figure 1*a* that the resonance complexes are highly resolved and the background contribution in the DR region is negligible. The resolution in σ_{RC} is remarkable given that it entails extremely detailed photoionization cross sections of hundreds of bound levels of Fe XVII. The cross sections have been radiatively damped; the effect has been found to be much smaller than for H- and He-like ions (Pradhan & Zhang 1997; Z99). The resonance structures are resolved to convergence in the final rates. This required calculations at extremely fine energy meshes up to 10^{-4} eV for individual resonance complexes up to $n = 10$.

The nearly fully resolved cross sections exhibit considerably more detail than the beam-averaged cross sections in the experiment on the Heidelberg heavy-ion storage ring (Savin et al. 1999). For the illustrative comparison in Figure 1*b*, we convolve the theoretical $v\sigma_{RC}$ with a Gaussian of FWHM 0.020 eV. As the DR high-*n* resonances are extremely narrow, we use theoretically averaged DR cross sections computed analytically from the Bell & Seaton (1985) theory to obtain the rate coefficients in the region $10 < \nu \le \infty$ below the $2s2p^6(^2S_{1/2})$ threshold. At low energies as $E \to 0$, the $\langle v\sigma_{RC}\rangle$ in

[2] See http://physics.nist.gov.

Figure 1*b* are somewhat lower than the experimental values since the former include the nonresonant background up to $n \leq 10$, $J \leq 7$. However, the resonance complexes $n =$ 18–20 (and higher) in the near-threshold region have been resolved (not shown for brevity), as in the inset in the lower panel showing experimental results. In the region $E < 12.7$ eV, the nonresonant RR-type contribution dominates over the resonant DR-type contribution (see Fig. 2*a* and related discussion). Although the Gaussian tends to accentuate the peaks rather more sharply, the agreement in resonance heights, positions, and shapes of the $n = 6$–10 complexes appears generally quite good (different values of FWHM up to 0.050 eV produce little basic change). The experimental beam shape is simulated by a "flattened" Maxwellian function with velocity components transverse and parallel to the beam (e.g., Kilgus et al. 1992), which is then used to fit and extract "resonance strengths" (Savin et al. 1999). While these may be compared with theory, a more precise comparison including the nonresonant background is now possible with the unified cross sections since the experiment also measures the same values. But because the theoretical results are more detailed, and owing to extremely narrow widths of resonances, the precise beam shape function needs to be used for convolution as in the experiment. However, the resonance strengths may be compared independently of the beam shape function. For example, we find that the integrated cross section $\sigma_{\rm RC}$ for the $n = 7$ complex is 350.7 (10^{-21} cm^2 eV), compared to the MCDF value of 335.7 and experimental value of 412.0 $\pm$ 8.1. More detailed comparisons will be presented in a later report.

As mentioned earlier, the peak of the DR cross section is theoretically equal to the threshold electron impact excitation cross section for the associated dipole core transition. The computed DR collision strength at the $^2S_{1/2}$ threshold is 0.27, in agreement with the electron impact excitation collision strength (Berrington & Pelan 2000 obtain 0.2882). The DR peak in Figure 1*b* is shown with the experimentally determined field ionization cutoff at $n_{\rm cut} \approx 124$; the $\langle v\sigma \rangle$ value is 3.87, compared to 4.18 at the theoretical limit at $n = \infty$, a difference of about 8%, indicating the degree of field ionization of the DR peak in the ion storage ring.

Of practical interest in astrophysical models is the total (e + ion) recombination rate coefficient $\alpha_R(T)$, including resonant and nonresonant (RR + DR) contributions, at all temperatures of ionic abundance. We present the Maxwellian-averaged $\alpha_R(T)$ in Figure 2, using the computed (unconvolved) $\sigma_{\rm RC}$. Figure 2*a* presents the partial $\alpha_R(T)$, including exactly the unified $\sigma_{\rm RC}$ as in Figure 1*a* (without the high-n "top-up" up to infinity, as in Fig. 2*b*), compared with the experimental DR results and the MCDF results (Savin et al. tabulate only the DR rates and blended resonance strengths). The partial unified $\alpha_R(T)$ in Figure 2*a* are significantly higher than the experimental DR-only rates because the nonresonant (RR-type) contribution monotonically rising toward low T as $E \rightarrow 0$ is included, together with the DR bump around 0.4 eV due to the $^2P^o_{1/2}nl$ resonances. The experimental recombination cross sections also reflect these two features. The MCDF results are seen to underestimate DR somewhat.

Finally, Figure 2*b* presents the total unified $\alpha_R(T)$ for Fe XVII (*solid curve*), using the calculated (unconvolved) cross sections and including a top-up nonresonant background contribution for recombination into Rydberg levels $11 \leq n \leq \infty$ computed in the hydrogenic approximation (e.g., N00; N01). In order to compare precisely with experimental DR results, we fit and add to it the nonresonant background contribution

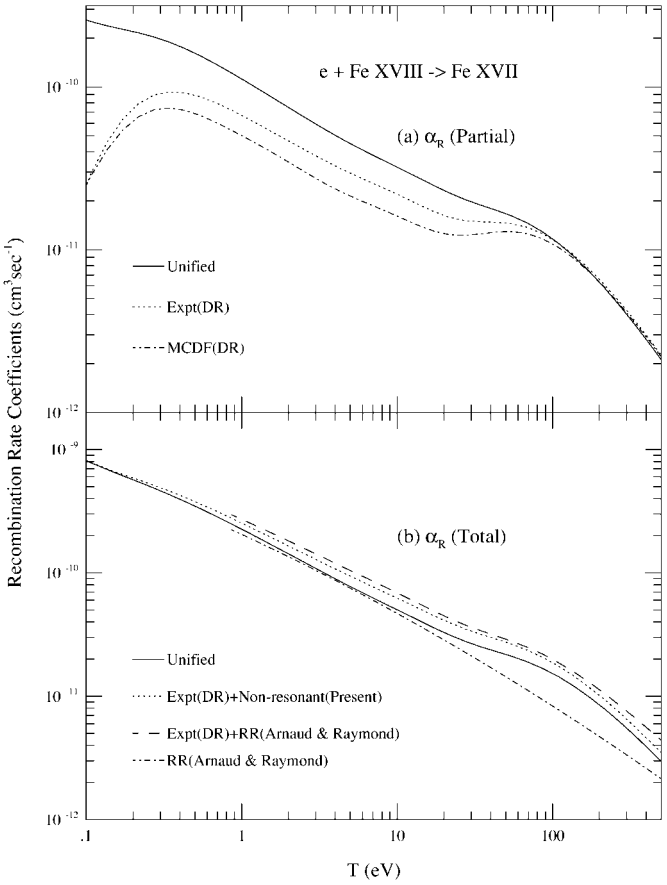

FIG. 2.—Unified recombination rate coefficients $\alpha_R(T)$ using computed $\sigma_{\rm RC}$. (*a*) Partial α_R corresponding to Fig. 1, compared with the experimental DR-only rates and multiconfiguration Dirac-Fock DR rates in Savin et al. (1999). The unified $\alpha_R(T)$ are significantly higher since they include the nonresonant background (including the low-T DR bump at ~0.4 eV). (*b*) Total $\alpha_R(T)$ compared with the sum of the experiment (DR) and the present nonresonant background (RR-type). The agreement is ~20%. Comparison with the sum of the experiment (DR) and RR (Arnaud & Raymond 1992) is also shown.

from the present total $\sigma_{\rm RC}$ (Fig. 1*a*). The difference of ~20% between the unified α_R and this sum ("experimental [DR] + nonresonant") is then almost entirely due to DR. Also shown is the sum of the experimental DR and the theoretical RR rate from Arnaud & Raymond (1992). Although a small contribution may still be unaccounted for, owing to resolution or high partial waves, the unified and the experimental results are within theoretical or experimental uncertainties.

We also calculated DR via the forbidden $^2P^o_{3/2}$–$^2P^o_{1/2}$ $M1$ core transition in Fe XVIII. Its contribution is negligible, although it may be of some consequence in other heavy, highly charged ions (Pradhan 1983) since $A(E2, M1)$ increases at much higher powers of Z than $A(E1)$.

4. DISCUSSION AND CONCLUSION

Astrophysical X-ray plasmas may be photoionized and/or collisionally ionized. Modeling of X-ray sources therefore requires total electronic recombination cross sections and rates at a wide range of energies and temperatures. To that end, we calibrate the unified theoretical and experimental data for recombination to Fe XVII against each other; we find good agreement in the low-energy region accessible experimentally. All other previous unified BPRM calculations have also shown

very good agreement with experiments for few-electron recombined ions C IV, C V, O VII (Z99), Ar XIV (Zhang & Pradhan 1997), and Fe XXIV (Pradhan & Zhang 1997). Unified recombination cross sections including resonant and nonresonant processes (RR and DR) may therefore be computed for most astrophysically abundant elements.

In the future, given the accuracy and resolution of the unified cross sections and possible partial delineation according to n, l, and J, an exact comparison with experimental measurements might yield precise information on (1) the missing background nonresonant (RR) contribution near threshold as $E \rightarrow 0$, into high Rydberg levels, (2) extraneous background contribution such as that due to charge transfer, and (3) high Rydberg resonances contributing to the DR peak and a more accurate field ionization cutoff than the approximate formulae heretofore employed.

Whereas the detailed comparison with experimental results (Fig. 1) for low-energy $\Delta n = 0$ ($E \leq 140$ eV) recombination is a useful test of accuracy, and relevant to low-T photoionized sources, collisionally ionized (coronal) high-T sources require total recombination rate coefficients up to $T = 10^8$ K (Arnaud & Raymond 1992). That, in turn, requires recombination cross sections up to $E \approx 1$ keV or higher. In fact, we may predict that the next DR peak at about 800 eV due to the $n = 3$ levels will be much bigger than at $^2S_{1/2}$ (Fig. 1), since there are several strong dipole transitions with A-values about 1–2 orders of magnitude higher than $A(^2S_{1/2} \rightarrow {}^2P^o_{3/2,\,1/2})$. The first set of these resonances begins at just above 400 eV, close to the temperature of maximum abundance of Fe XVII in coronal equilibrium. Correspondingly, there will be a higher peak in the recombination rate than the one around 100 eV (Fig. 2). The $\Delta n = 1$ DR therefore is expected to contribute more to total electronic recombination of (e + Fe XVIII) $\rightarrow$ Fe XVII than the $\Delta n = 0$ core transitions. The higher energy unified recombination calculations are in progress.

One of the main points is that since photoionization and recombination are treated as inverse processes with the same eigenfunction expansion for the core ion (eq. [1]), the same set of resonances and nonresonant background are included in both processes—an essential requirement for self-consistency in photoionization equilibrium, as expressed by

$$\int_{\nu_0}^{\infty} \frac{4\pi J_\nu}{h\nu} N(X^z)\sigma_{\rm PI}(\nu, X^z)d\nu = \sum_j N_e N(X^{z+1})\alpha_R(X^z_j;\ T), \quad (2)$$

where $\sigma_{\rm PI}$ is the photoionization cross section and J_ν is the radiation flux. In general, the sum on the right-hand side of equation (2) extends over the infinite number of recombined bound levels. Now, if the α_R on the right-hand side is subdivided into nonresonant RR and resonant DR, as in existing photoionization models, then fundamental inconsistencies result. The RR rate is supposedly derived from nonresonant photoionization cross sections. But as we see from Figure 1, the near-threshold region is dominated by resonances and a rising nonresonant background. Therefore, photoionization calculations must also be carried out including the same resonances (see the Opacity Project work; Seaton et al. 1994 and references therein). The issue of radiative transfer and resonance positions may be ameliorated by (1) averaging over the radiation field on the left-hand side of equation (2), and (2) preaveraging over resonances in photoionization cross sections (Bautista, Romano, & Pradhan 1998). The further subdivision of DR into $\Delta n = 0$ rates (as, for example, derived experimentally by Savin et al. 1999) appropriate only for low-T plasmas, and $\Delta n > 0$ DR needed in high-T plasmas, implies that the recombination rates must be obtained for RR + DR ($\Delta n = 0$) + DR($\Delta n > 0$), generally using different approximations and possibly valid in different temperature regimes. The problems with this—(1) inconsistent photoionization and recombination, (2) unphysical division of RR and DR, and (3) low- and high-energy DR in different but overlapping energy (temperature) ranges—may be overcome with the unified method for electronic recombination and corresponding photoionization cross sections to enable a self-consistent treatment of photoionization and recombination in X-ray photoionized sources.

We would like to thank Werner Eissner for invaluable assistance with the BPRM codes. This work was partially supported by the NSF and the NASA Astrophysical Theory Program.

REFERENCES

Arnaud, M., & Raymond, D. 1992, ApJ, 398, 394
Bautista, M. A., Romano, P., & Pradhan, A. K. 1998, ApJS, 118, 259
Bell, R. H., & Seaton, M. J. 1985, J. Phys. B, 18, 1589
Berrington, K. A., Eissner, W., & Norrington, P. H. 1995, Comput. Phys. Commun., 92, 290
Berrington, K. A., & Pelan, J. 2000, A&AS, in press
Brickhouse, N., Raymond, J. C., & Smith, B. W. 1995, ApJS, 97, 551
Burke, P. G., Hibbert, A., & Robb, D. 1971, J. Phys. B, 4, 153
Canizares, C. R., et al. 2000, in Atomic Data Needs in X-Ray Astronomy, ed. M. A. Bautista, T. R. Kallman, & A. K. Pradhan (NASA CP-2000-209968; Greenbelt: NASA), 5
Eissner, W., Jones, M., & Nussbaumer, H. 1974, Comput. Phys. Commun., 8, 270
Fabian, A. C., Mushotzky, R. F., Nulsen, P. E. J., & Peterson, J. R. 2001, MNRAS, 321, L20
Hummer, D. G., Berrington, K. A., Eissner, W., Pradhan, A. K., Saraph, H. E., & Tully, J. A. 1993, A&A, 279, 298
Kallman, T. 1995, in AIP Conf. Proc. 547, Atomic Processes in Plasmas, ed. R. C. Mancini & R. A. Phaneuf (New York: AIP), 36
Kilgus, G., Habs, D., Schwalm, D., Wolf, A., Badnell, N. R., & Müller, A. 1992, Phys. Rev. A, 46, 5730
Mannervik, S., Asp, S., Broström, L., DeWitt, D. R., Lidberg, L., Schuch, R., & Chung, K. T. 1997, Phys. Rev. A, 55, 1810
Nahar, S. N., & Pradhan, A. K. 1994, Phys. Rev. A, 49, 1816 (NP94)
Nahar, S. N., Pradhan, A. K., & Zhang, H. L. 2000, ApJS, 131, 375 (N00)
———. 2001, ApJS, 133, 255 (N01)
Ogle, P. M., Marshall, H. L., Lee, J. C., & Canizares, C. R. 2000, ApJ, 545, L81
Pradhan, A. K. 1983, Phys. Rev. A, 28, 2128
Pradhan, A. K., & Zhang, H. L. 1997, J. Phys. B, 30, L571
Predehl, P., et al. 2000, in Atomic Data Needs in X-Ray Astronomy, ed. M. A. Bautista, T. R. Kallman, & A. K. Pradhan (NASA CP-2000-209968; Greenbelt: NASA), 11
Savin, D. W., et al. 1997, ApJ, 489, L115
———. 1999, ApJS, 123, 687
Schulz, N. S., Canizares, C. R., Husenmoerder, D., & Lee, J. C. 2000, ApJ, 545, L135
Scott, N. S., & Taylor, K. T. 1982, Comput. Phys. Commun., 25, 347
Seaton, M. J., Yan, Y., Mihalas, D., & Pradhan, A. K. 1994, MNRAS, 266, 805
Zhang, H. L., Nahar, S. N., & Pradhan, A. K. 1999, J. Phys. B, 32, 1459 (Z99)
Zhang, H. L., & Pradhan, A. K. 1997, Phys. Rev. Lett., 78, 195